Direct extraction of Raman line-shapes from congested CARS spectra

Erik M. Vartiainen

Department of Electrical Engineering, Lappeenranta University of Technology, B.O. Box 20, FI-53851 Lappeenranta, Finland
Erik.Vartiainen@lut.fi

Hilde A. Rinia and Michiel Müller

Swammerdam Institute for Life Sciences, University of Amsterdam, P.O. Box 94062, 1090 GB Amsterdam, The Netherlands
rinia@science.uva.nl, muller@science.uva.nl

Mischa Bonn

FOM Institute for Atomic and Molecular Physics [AMOLF], Kruislaan 407 Amsterdam, The Netherlands
m.bonn@amolf.nl

Abstract: We show that Raman line-shapes can be extracted directly from congested coherent anti-Stokes Raman scattering (CARS) spectra, by using a numerical method to retrieve the phase-information hidden in measured CARS spectra. The proposed method utilizes the maximum entropy (ME) model to fit the CARS spectra and to further extract the imaginary part of the Raman susceptibility providing the Raman line-shape similar to the spontaneous Raman scattering spectrum. It circumvents the challenges arising with experimentally determining the real and imaginary parts of the susceptibility independently. Another important advantage of this method is that no *a priori* information regarding the vibrational resonances is required in the analysis. This permits, for the first time, the quantitative analysis of CARS spectra and microscopy images without any knowledge of e.g. sample composition or Raman response.

©2006 Optical Society of America

OCIS codes: (300.6230) Spectroscopy, coherent anti-Stokes Raman scattering; (000.3860) General, mathematical methods in physics.

References and links

1. G. R. Holtom, B. D. Thrall, B. Chin, and D. Colson, "Achieving molecular selectivity in imaging using multiphoton Raman spectroscopy techniques," Traffic **2**, 781-788 (2001).
2. J. X. Cheng and X. S. Xie, "Coherent Anti-Stokes Raman Scattering Microscopy: Instrumentation, Theory, and Applications," J. Phys. Chem. B **108**, 827-840 (2004).
3. A. Volkmer, "Vibrational imaging and microspectroscopies based on coherent anti-Stokes Raman scattering microscopy," J. Phys. D: Appl. Phys. **38**, R59-R81 (2005).
4. G. J. Puppels, F. F. M. de Mul, C. Otto, J. Greve, M. Robert-Nicoud, D. J. Arndt-Jovin, and T. M. Jovin, "Studying single living cells and chromosomes by confocal Raman microspectroscopy," Nature **347**, 301-303 (1990).
5. H. van Manen, Y. M. Kraan, D. Roos, and C. Otto, "Single-cell Raman and fluorescence microscopy reveal the association of lipid bodies with phagosomes in leukocytes," Proc. Natl. Acad. Sci. USA **102**, 10159-10164 (2005).
6. M. Müller and J. M. Schins, "Imaging the thermodynamic state of lipid membranes with multiplex CARS microscopy," J. Phys. Chem. B **106**, 3715-3723 (2002).
7. G. W. H. Wurpel, J. M. Schins, and M. Müller, "Chemical specificity in 3D imaging with multiplex CARS microscopy," Opt. Lett. **27**, 1093-1095 (2002).
8. J. X. Cheng, A. Volkmer, L. D. Book, and X. S. Xie, "Multiplex coherent anti-Stokes Raman scattering microspectroscopy and study of lipid vesicles," J. Phys. Chem. B **106**, 8493-8498 (2002).

#68664 - $15.00 USD Received 3 March 2006; revised 30 March 2006; accepted 1 April 2006

9. M. Müller, J. M. Schins, and G. W. H. Wurpel, "Shot-noise limited detection sensitivity in multiplex CARS microscopy," SPIE **5323**, 195-204 (2004).
10. G. W. H. Wurpel, J. M. Schins, and M. Müller, "Direct measurement of chain order in single lipid mono- and bilayers with multiplex CARS," J. Phys. Chem. B **108**, 3400-3403 (2004).
11. S. A. Akhmanov, A. F. Bunkin, S. G. Ivanov, and N. I. Koroteev, "Polarization active Raman spectroscopy and coherent Raman elipsometry," Sov. Phys. JETP **47**, 667-678 (1978).
12. J. Cheng, L. D. Book, and X. S. Xie, "Polarization coherent anti-Stokes Raman scattering microscopy," Opt. Lett. **26**, 1341-1343 (2001).
13. A. Volkmer, L. D. Book, and X. S. Xie, "Time-resolved coherent anti-Stokes Raman scattering microscopy: imaging based on Raman free induction decay," Appl. Phys. Lett. **80**, 1505-1507 (2002).
14. D. Oron, N. Dudovich, D. Yelihn, and Y. Silberberg, "Quantum control of coherent anti-Stokes Raman processes," Phys. Rev. A **65**, 43408-1/4 (2002).
15. D. Oron, N. Dudovich, and Y. Silberberg, "Femtosecond Phase-and-Polarization Control for Background-Free Coherent Anti-Stokes Raman Spectroscopy," Phys. Rev. Lett. **90**, 213902 (2003).
16. A. Volkmer, J. Cheng, and X. S. Xie, "Vibrational imaging with high sensitivity via epidetected coherent anti-Stokes Raman scattering microscopy," Phys. Rev. Lett. **87**, 23901 (2001).
17. J. Cheng, A. Volkmer, L. D. Book, and X. S. Xie, "An epi-detected coherent anti-Stokes Raman scattering (E-CARS) microscope with high spectral resolution and high sensitivity," J. Phys. Chem. B **105**, 1277-1280 (2001).
18. H. A. Rinia, M. Bonn, and M. Müller, "Quantitative multiplex CARS spectroscopy in congested spectral regions," J. Phys. Chem. B **110**, 4472-4479 (2006).
19. F. Y. Yueh and E. J. Beiting, "Simultaneous N_2, CO, and H_2 multiplex CARS measurements in combustion environments using a single dye laser," Appl. Opt. **27**, 3233-3243 (1988).
20. C. F. Kaminski and P. Ewart, "Multiplex H_2 coherent anti-Stokes Raman scattering thermometry with a modeless laser," Appl. Opt. **36**, 731-734 (1997).
21. C. Otto, A. Voroshilov, S. G. Kruglik, and J. Greve, "Vibrational bands of luminescent zinc(II)-octaethyl-porphyrin using a polarization-sensitive 'microscopic' multiplex CARS technique," J. Raman Spectrosc. **32**, 495-501 (2001).
22. D. Oron, N. Dudovich, and Y. Silberberg, "Single-pulse phase-contrast nonlinear Raman spectroscopy," Phys. Rev. Lett. **89**, 27300 (2002).
23. S. Lim, A. G. Caster, and S. R. Leone, "Single-pulse phase-control interferometric coherent anti-Stokes Raman scattering spectroscopy," Phys. Rev. A **72**, 41803 (2005).
24. E. O. Potma, C. L. Evans and X. S. Xie, "Heterodyne coherent anti-Stokes Raman scattering (CARS) imaging," Opt. Lett. **31**, 241-243 (2006).
25. D.L. Marks, C. Vinegoni, J.S. Bredfeldt and S.A. Boppart, "Interferometric differentiation between resonant coherent anti-Stokes Raman scattering and nonresonant four-wave-mixing processes," Appl. Phys. Lett. **85**, 5787-5789 (2004).
26. E. M. Vartiainen, "Phase retrieval approach for coherent anti-Stokes Raman scattering spectrum analysis," J. Opt. Soc. Am. B **9**, 1209-1214 (1992).
27. E. M. Vartiainen, K.-E. Peiponen, and T. Asakura, "Phase retrieval in optical spectroscopy: resolving optical constants from power spectra," Appl. Spectrosc. **50**, 1283-1289 (1996).
28. R. A. MacPhail, H. L. Strauss, R. G. Snyder, and C. A. Elliger, "Carbon-hydrogen stretching modes and the structure of n-alkyl chains. 2. Long, all-trans chains," J. Phys. Chem. **88**, 334-341 (1984).
29. R. Mendelsohn and D. J. Moore, "Vibrational spectroscopic studies of lipid domains in biomembranes and model systems," Chem. Phys. Lipids **96**, 141-157 (1998).
30. K. T. Yue, C. L. Martin, D. Chen, P. Nelson, D. L. Sloan, and R. Callender, "Raman spectroscopy of oxidized and reduced nicotinamide adenine dinucleotides," Biochem **25**, 4941-4947 (1986).
31. L. Rimai, T. Cole, J. L. Parsons, J. T. Hickmott, Jr., and E. B. Carew, "Studies of Raman spectra of water solutions of Adenosine tri-, di-, and monophosphate and some related compounds," Biophys. J. **9**, 320-329 (1969).
32. R. H. Jenkins, R. Tuma, J. T. Juuti, D. H. Bamford and J. J. Thomas, "A novel Raman spectrophotometric method for quantitative measurement of nucleoside triphosphate hydrolysis," Biospectroscopy **5**, 3-8 (1999).

1. Introduction

Enabled by recent short-pulse laser technology developments, coherent anti-Stokes Raman scattering (CARS) microscopy is being used increasingly as a unique microscopic tool in biophysics, biology and the material sciences [1-3]. As a non-linear optical analogue of spontaneous Raman scattering, CARS potentially provides image contrast with chemical and

#68664 - $15.00 USD Received 3 March 2006; revised 30 March 2006; accepted 1 April 2006
(C) 2006 OSA

physical specificity, since many of the important vibrational spectral features remain resolvable even at room temperature and in samples as complex as live cells [1, 4, 5].

To fully exploit the unique potential of CARS microscopy, CARS spectra with a high signal-to-noise ratio (SNR) are required. This can be accomplished in a multiplex CARS approach [6, 7, 8], where a significant part of the vibrational spectrum is measured concurrently by using a combination of a broad-band and narrow-band laser sources. The SNR of the acquired multiplex CARS spectra in this case is limited only by Poisson noise [9, 10].

Due to the coherent addition of both resonant contributions from different vibrational modes and a non-resonant (NR) background contribution, CARS spectra generally have a complex shape. The influence of the NR background can be significantly reduced using various methods [11-17]. However, by using the NR background - rather than suppressing it, the resonant contribution to the multiplex CARS spectrum can be measured relative to the NR background, yielding a CARS signal strength which is independent of experimental parameters such as laser power, acquisition time, alignment, etc. and can therefore be related quantitatively to the concentration of the molecular species of interest [9, 18]. Also, the use of the NR contribution increases the detection sensitivity through a heterodyne type amplification of the resonant contribution.

Multiplex CARS spectroscopy is widely used for temperature and composition measurements in combustion environments and plasma (see e.g. [19, 20]). These spectra are generally characterized by well-separated vibrational resonances. Multiplex CARS spectroscopy has also been used in the study of the vibrational structure of protein complexes under resonant excitation conditions, where the different non-linear susceptibility tensor elements have been analyzed separately using polarization sensitive techniques [21]. In the latter case, like for biological samples in general, elaborate data analysis based on a priori knowledge of the vibrational (Raman) spectrum is generally required to extract the information contained in the CARS spectra, in particular when attempting to quantify different constituents [18]. However, problems arise when investigating unknown samples, because in that case knowledge concerning the Raman spectra of the present components is not available. This complication arises from the fact that the CARS intensity as such is not a direct measure of the concentration of individual components, and the conversion of CARS to Raman data is essential for extracting quantitative information from CARS spectra. This drawback can be circumvented by determining experimentally both the real and imaginary component of the third-order non-linear susceptibility that is responsible for the CARS signal. Recently several elegant approaches have been developed to simultaneously measure the real and imaginary part of the CARS spectrum [22-25]. These sophisticated methods rely on spectral interferometry and require experimental control over the phase of the laser pulses employed in the experiments.

In this paper, we present an alternative approach to determine the magnitude and phase directly from measured multiplex CARS spectra. This method does not require any a priori information on the vibrational resonance structure of the sample, in order to extract quantitative spectral information from multiplex CARS spectra in congested spectral regions, and is in principle applicable to any CARS spectrum of sufficient signal-to-noise ratio. It employs the maximum entropy (ME) method to retrieve the phase function of the non-linear susceptibility tensor elements, $\chi^{(3)}_{ijkl}$, responsible for the CARS line-shape. Knowledge of this phase function permits full retrieval of the spectral information - contained in the imaginary part of $\chi^{(3)}_{ijkl}$ - otherwise hidden in the complex shape of the CARS spectrum due to the coherent nature of this non-linear process.

We have applied this novel method to CARS spectra of 1,2-dimyristoyl-*sn*-glycero-3-phosphocholine (DMPC), a common phospholipid, and adenosine mono-, di and triphosphate (AMP, ADP and ATP), which are nucleotides involved in many different energy-driven biological reactions. These molecules can be regarded as representative biological samples exhibiting congested spectra. We found that the imaginary part of the Raman susceptibility, as

#68664 - $15.00 USD Received 3 March 2006; revised 30 March 2006; accepted 1 April 2006
(C) 2006 OSA

retrieved from the CARS spectra by the ME method, shows excellent agreement with the actual measured Raman spectra, validating this method as a faithful means to extract spectral information from CARS measurements. This method permits a quantitative interpretation of CARS spectra without previous knowledge of the Raman spectra.

2. Theory

The multiplex CARS signal is given by

$$I_{CARS}(\omega_{as}) \propto \left|P^{(3)}(\omega_{as})\right|^2 = \left|E_{pu}\right|^2 \left|E_{pr}\right|^2 \left|E_S(\omega_{as})\right|^2 \left|\chi^{(3)}_{1111}(-\omega_{as};\omega_{pu},-\omega_S,\omega_{pr})\right|^2 \qquad (1)$$

where $P^{(3)}(\omega_{as})$ is the induced third-order polarization, E_{pu} and E_{pr} are the pump and probe electric fields, $E_S(\omega_{as})$ is the Stokes electric field and $\chi^{(3)}_{1111}(-\omega_{as};\omega_{pu},-\omega_S,\omega_{pr})$ is the component of the third-order susceptibility, which is relevant for the experimental circumstances of parallel polarization conditions. Away from one-photon resonances $\chi^{(3)}_{1111}$ can be considered as the sum of a NR part ($\chi^{(3)}_{NR}$) arising from the electronic contributions and a Raman resonant part ($\chi^{(3)}_{R}$) as:

$$\chi^{(3)}_{1111}(\omega_{as}) = \chi^{(3)}_{NR} + \chi^{(3)}_{R}(\omega_{as}) \qquad (2)$$

where the NR part is purely real and frequency independent. The resonant part is a complex function and can be written as

$$\chi^{(3)}_{R}(\omega_{as}) = \sum_j \frac{A_j}{\Omega_j - (\omega_{pu} - \omega_S) - \mathrm{i}\,\Gamma_j} \qquad (3)$$

where A_j , Ω_j and Γ_j are the amplitude, the frequency and the line-width of *j*'th Raman mode, respectively. In the experiment the CARS signal from the sample is divided by the CARS signal from a reference sample that has no vibrational resonances over the frequency range of the measurement. Thereby, the obtained CARS line-shape, $S(\omega_{as})$, is directly proportional to the squared modulus of $\chi^{(3)}_{1111}$ as:

$$S(\omega_{as}) = \frac{\left|\chi^{(3)}_{NR} + \chi^{(3)}_{R}(\omega_{as})\right|^2}{\left|\chi^{(3)}_{NR,ref}\right|^2} = \left|\chi_{nr} + \chi_r(\omega_{as})\right|^2 = \chi^2_{nr} + 2\chi_{nr}\,\mathrm{Re}\left[\chi_r(\omega_{as})\right] + \left|\chi_r(\omega_{as})\right|^2 \qquad (4)$$

where $\chi_{nr} = \chi^{(3)}_{NR} / \chi^{(3)}_{NR,ref}$ is normalized background term and $\chi_r(\omega_{as}) = \chi^{(3)}_{R}(\omega_{as}) / \chi^{(3)}_{NR,ref}$ is a normalized Raman resonant term given by equation (3). Since $\mathrm{Re}\left[\chi_r(\omega_{as})\right]$ has a dispersive line-shape and $\left|\chi_r(\omega_{as})\right|^2$ in turn a dissipative line-shape, retrieval of the spectral information contained in the CARS spectrum requires knowledge of the imaginary part, or the phase function, of $\chi_r(\omega_{as})$.

In comparison, the spontaneous Raman scattering line-shape is given by the imaginary part of the linear Raman susceptibility, $\chi^{(1)}_{R}$, as

$$I_{Raman}(\omega) \propto -\mathrm{Im}\left[\chi^{(1)}_{R}(\omega)\right] = \sum_j \frac{A_j \Gamma_j}{(\Omega_j - \omega)^2 + \Gamma_j^2} \qquad (5)$$

#68664 - $15.00 USD Received 3 March 2006; revised 30 March 2006; accepted 1 April 2006
(C) 2006 OSA

Hence, it is obvious from comparing equations (3) and (5) that both the imaginary part of $\chi_r(\omega_{as})$ within the complex CARS line-shape and the spontaneous Raman line-shape contain the same spectral information and are directly comparable.

In this work, our goal is to extract the spontaneous Raman line-shape from the CARS line-shape, i.e. $\mathrm{Im}\,\chi_r(\omega_{as})$, without making any assumptions regarding the Raman lines (i.e., the vibrational frequencies, line-widths and amplitudes). Instead, we fit the CARS line-shape with the ME model and use it to estimate the phase function, $\theta_r(\omega_{as}) = \arg\{\chi_r(\omega_{as})\}$, of the Raman susceptibility. The ME model for the CARS line-shape function, $S(\omega_{as})$, is given by [26]

$$S(v) = \left| \frac{\beta}{1 + \sum_{k=1}^{M} a_k \exp(-2\pi \mathrm{i}\, kv)} \right|^2 = \left| \frac{\beta}{A_M(v)} \right|^2 \tag{6}$$

where ν is a normalized frequency defined by the selected lower ($\omega_{\min} = \min\{\omega_{as}\}$) and upper ($\omega_{\max} = \max\{\omega_{as}\}$) limits of the CARS spectrum as:

$$v = \frac{\omega_{as} - \omega_{\min}}{\omega_{\max} - \omega_{\min}} \tag{7}$$

The ME coefficients a_k and $|\beta|$ can be solved from a (Toeplitz) set of linear equations:

$$\begin{bmatrix} C_0 & C_1^* & \cdots & C_M^* \\ C_1 & C_0 & \cdots & C_{M-1}^* \\ \vdots & \vdots & \ddots & \vdots \\ C_M & C_{M-1} & \cdots & C_0 \end{bmatrix} \begin{bmatrix} 1 \\ a_1 \\ \vdots \\ a_M \end{bmatrix} = \begin{bmatrix} |\beta|^2 \\ 0 \\ \vdots \\ 0 \end{bmatrix} \tag{8}$$

where (*) denotes the complex conjugate, and the coefficients, C_m, are given by the (discrete) Fourier transform of the CARS line-shape at a discrete set of the normalized frequencies $v_j = j/L$ ($j = 0, 1, \ldots, L$):

$$C_m = L^{-1} \sum_{j=0}^{L-1} S(v_j) \exp(2\pi \mathrm{i}\, m \nu_j) \tag{9}$$

We define the ME phase function, $\psi(v) = \arg\{A_M(v)\}$, connected to the polynomial in equation (6). This phase is the key element in the retrieval of the true phase, $\theta(v) = \arg(\chi_{nr} + \chi_r)$, from the CARS line-shape. Using equation (6) we can write:

$$\chi_{nr} + \chi_r(v) = \sqrt{S(v)}\, \exp[\mathrm{i}\,\theta(v)] \cong \frac{|\beta| \exp[\mathrm{i}\,\theta(v)]}{|A_M(v)|} = \frac{|\beta| \exp[\mathrm{i}\,\theta(v) - \mathrm{i}\,\psi(v)]}{A_M(v) \exp[-\mathrm{i}\,\psi(v)]} = \frac{|\beta| \exp[\mathrm{i}\,\varphi(v)]}{A_M^*(v)} \tag{10}$$

where we introduce an error phase, $\varphi(v) = \theta(v) - \psi(v)$, as the difference between the true and the ME phase. The idea behind using the ME model for phase retrieval is the fact that $\psi(v)$ includes the same spectral features as $\theta(v)$, whereas $\varphi(v)$ provides a slowly varying background term to $\theta(v)$ [27]. Thus, the phase retrieval problem reduces to performing a background correction to $\psi(v)$. In case the CARS spectrum consists of a weak resonant structure embedded on a large background, i.e. $\mathrm{Im}\,\chi_r(v) << (\chi_{nr} + \mathrm{Re}\,\chi_r(v))$, the constraint:

#68664 - $15.00 USD Received 3 March 2006; revised 30 March 2006; accepted 1 April 2006
(C) 2006 OSA

$$\theta(\nu) = \tan^{-1}\left[\frac{\mathrm{Im}\,\chi_r(\nu)}{\chi_{nr} + \mathrm{Re}\,\chi_r(\nu)}\right] \approx 0 \tag{11}$$

holds, when ν is removed from any of the resonances. In the following we utilize solely this constraint to estimate and to establish the phase function:

$$\theta(\nu) \approx \theta_{\mathrm{est}}(\nu) = \varphi_{\mathrm{est}}(\nu) + \psi(\nu) \tag{12}$$

allowing us to deduce the Raman line-shape as:

$$\mathrm{Im}\left[\chi_r(\nu)\right] \approx \sqrt{S(\nu)}\ \ \sin\theta_{\mathrm{est}}(\nu) \tag{13}$$

3. Experimental

The experimental set-up for multiplex CARS has been described in detail elsewhere (see [6, 17]). Briefly, a 10 ps (bandwidth 1.5 cm^{-1} full width at half maximum (fwhm)) pump/probe laser at 710 nm is overlapped, in time and space, with a 80 fs (bandwidth ~180 cm^{-1} fwhm) Stokes laser. The Stokes laser is tunable between 750 and 950 nm, corresponding to a vibrational range of ~750-3500 cm^{-1}. For the experimental results presented here, the laser beams are focused with an achromatic lens (f = 5 cm) in a tandem cuvet. The cuvet can be translated perpendicular to the optical axis to measure the signal in either of the two compartments, providing a multiplex CARS spectrum of the sample and of a (non-resonant) reference. Typical laser powers are 75 mW and 105 mW for the pump/probe and Stokes laser respectively. The generated anti-Stokes signal is filtered and spectrally resolved on a spectrometer with an effective spectral resolution of ~5 cm^{-1}. Achromatic λ/2 plates and polarizers ensure all-parallel polarization conditions for pump, Stokes, probe and anti-Stokes. All multiplex CARS spectra shown have an acquisition time of 800 ms.

Spontaneous Raman scattering spectra are measured with a Raman microscope (Renishaw RM1000, spectral resolution: ~5 cm^{-1}) equipped with a 6 mW HeNe laser. A polarizer in the detection channel ensures that only scattered light is detected with a plane of polarization parallel to that of the exciting radiation. Acquisition times are 2 and 3 minutes for the DMPC lipid sample and the AMP/ADP/ATP mixture, respectively.

#68664 - $15.00 USD Received 3 March 2006; revised 30 March 2006; accepted 1 April 2006
(C) 2006 OSA

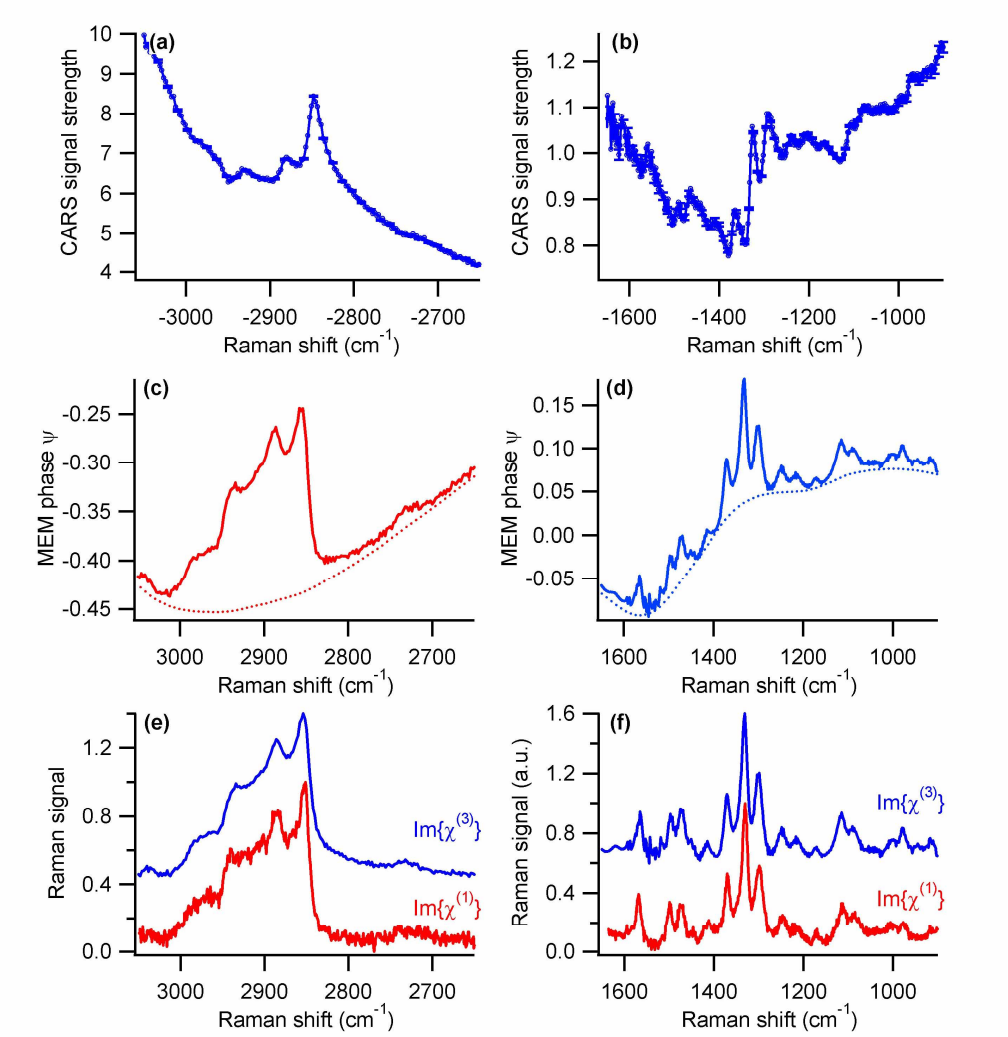

Fig. 1. The CARS line-shapes in the vicinity of vibrational resonances of DMPC (a) and ADP/AMP/ATP (b). The corresponding ME phases, $\psi(\omega)$, (solid lines) and the estimated background phase, $-\varphi_{est}(\omega)$, (dotted lines) of DMPC (c) and ADP/AMP/ATP (d). The Raman line-shapes obtained from CARS spectra (blue lines) and the corresponding spontaneous Raman scattering spectra (red lines) of DMPC (e) and ADP/AMP/ATP (f).

4. Results

As a first demonstration of the described phase retrieval technique for multiplex CARS spectra, we consider the results obtained for a 75 mM DMPC small unilamellar vesicles (SUV) suspension (Fig. 1). The assignment of most of the vibrational resonances in the CH-stretch region is known [28, 29]. Most prominent is the peak at 2847 cm^{-1}, which is due to the symmetric methylene stretch vibration. In total, at least eight vibrational resonances are required to fit the Raman spectrum of the lipid. In Fig. 1(a) the multiplex CARS line-shape of DMPC is displayed in the CH-stretch region between -2600 and -3100 cm^{-1}. In addition to the C-H stretch resonances, the CARS line-shape is strongly influenced by the broad vibrational response of water around -3300 cm^{-1}. This provides, in perspective of the present procedure, a non-constant, complex background to the spectrum. The corresponding ME-phase, ψ, is

#68664 - $15.00 USD Received 3 March 2006; revised 30 March 2006; accepted 1 April 2006
(C) 2006 OSA

shown in Fig. 1(c) (solid line) along with the estimated background phase (dotted line), $-\varphi_{\text{est}}$, which results from both the non-resonant background signal and the wing of the resonant line of water. If the influence of the varying background due to the water line was negligible, this background phase would be a constant. Nevertheless, the constraint of Eq. (11) still holds for the resonances of DMPC, and the estimate phase function, $-\varphi_{\text{est}}$, is obtained by cubic spline interpolation using solely Eq. (11) on the grounds that the amplitudes of the resonances in interest are small compared to the background signal. In practice, those regions where Eq. (11) is met (i.e. where the resonant signals are small) are included in the data to which a function is fitted. This means that those contributions to the phase function θ that do not result from the DMPC lipid resonances are all contained in the background phase $-\varphi_{\text{est}}$. Then, by subtracting the background phase from ψ, we get the phase estimate, $\theta_{\text{est}} = \varphi_{\text{est}} + \psi$. Using Eq. (13) the imaginary part, $\text{Im}\,\chi_r$, is obtained yielding directly the Raman line-shape of DMPC. This is demonstrated in Fig. 1(e) where the imaginary part obtained from the multiplex CARS spectrum (blue line) is shown with the spontaneous Raman scattering spectrum of DMPC (red line). It should be noted that the CARS spectrum was converted to the corresponding Raman spectrum without any information about the Raman spectrum to be expected.

A second example consists of a congested vibrational spectrum from an equimolar mixture of AMP, ADP and ATP in water for a total concentration of 500 mM. The adenine ring vibrations [30] are found at identical frequencies for either for AMP, ADP or ATP around 1350 cm^{-1}. The phosphate vibrations between 900 and 1100 cm^{-1} can be used to discriminate between the different nucleotides [18, 31, 32]. The tri-phosphate group of ATP shows a strong resonance at -1123 cm^{-1}, whereas the monophosphate resonance of AMP is found at -979 cm^{-1}. For ADP a broadened resonance is found in between at -1100 cm^{-1}. The measured multiplex CARS spectrum is shown in Fig. 1(b). Similar to the case of DMPC presented above, the ME-phase displays the resonant structure of molecular vibrations on top of a slowly varying background phase (Fig. 1(d)). Again, we estimate the background phase using Eq. (11) with spline fitting (Fig. 1(d), dotted line), and thereby compute the phase estimate and the Raman line-shape using Eqs. (12) and (13), respectively. The latter is shown in Fig. 1(f) (blue line) with the corresponding spectrum from spontaneous Raman scattering measurement (red line).

These two examples serve to illustrate that the procedure presented here allows for the direct conversion of CARS data into a Raman response, without prior knowledge of the Raman response itself, even for highly congested spectra. The conversion of CARS to Raman data permits a quantitative interpretation of CARS spectra of unknown samples [18].

5. Conclusions

By analyzing congested CARS line-shapes using the maximum entropy model a ME-phase function could be obtained. From the spectral regions where CARS resonance lines of interest are smaller than the background CARS signal, the background phase function is readily inferred. Correcting the ME-phase function for the background phase allows for the straightforward extraction of the inherent phase of the resonant CARS signal, which is identical to the Raman line-shape. In this paper, we demonstrate this approach on two very different samples. We have used a simple curve fitting to subtract the background from the ME-phase. After successful background subtraction the phase of the CARS signal, and thereby the Raman line-shape, of the vibrational moiety is obtained. Thus, no additional information other than the CARS signal itself is required to extract the Raman line-shape from the CARS measurement. The application of this method to two types of congested CARS spectra - solutions of DMPC phospholipid and an adenosine (mono-, di-, and tri-)phosphate mixture in water, reveals that in both cases the Raman line-shapes extracted from the CARS spectra show excellent agreement with the actual spontaneous Raman scattering spectra. In summary, we have demonstrated a method to extract the Raman line-shape from measured

#68664 - $15.00 USD Received 3 March 2006; revised 30 March 2006; accepted 1 April 2006
(C) 2006 OSA

CARS spectra, without a priori knowledge of the vibrational spectrum. This enables, for the first time, the interpretation of multiplex CARS images of samples with unknown composition.

Acknowledgment

This work is part of the research program of the 'Stichting voor Fundamenteel Onderzoek der Materie (FOM)', which is financially supported by the 'Nederlandse Organisatie voor Wetenschappelijk Onderzoek (NWO)'.

#68664 - $15.00 USD Received 3 March 2006; revised 30 March 2006; accepted 1 April 2006
(C) 2006 OSA